

# Rare nonleptonic $B_s$ -meson decays as a probe for new physics beyond the standard model

G. Faisel<sup>1</sup> and J. Tandean<sup>2</sup>

<sup>1</sup>Department of Physics, Faculty of Arts and Sciences, Süleyman Demirel University, Isparta 32260, Turkey

<sup>2</sup>Department of Physics, National Taiwan University, Taipei 106, Taiwan and Physics Division, National Center for Theoretical Sciences, Hsinchu 300, Taiwan

E-mail: [gaberfaisel@sdu.edu.tr](mailto:gaberfaisel@sdu.edu.tr), [jtandean@yahoo.com](mailto:jtandean@yahoo.com)

**Abstract.** The recent measurements on a number of  $b \rightarrow s\mu^+\mu^-$  processes have manifested anomalous results which could be early evidence for the presence of new physics beyond the standard model in  $b \rightarrow s$  transitions. Supposing this to be the case, we entertain the possibility that a heavy  $Z'$  boson is responsible for these anomalies and that it also affects the rare nonleptonic decays of the  $\bar{B}_s$  meson which receive substantial contributions from the so-called penguin diagrams. The majority of these  $\bar{B}_s$  decay modes are not yet discovered, and within the standard model their rates have been estimated to be relatively suppressed. Taking into account various constraints, we find that the  $Z'$  effects can enlarge the rates of a few of the modes, especially  $\bar{B}_s \rightarrow \eta\pi^0, \phi\pi^0, \eta\omega, \phi\omega$ , considerably above their standard-model expectations. Consequently this  $Z'$  scenario may be experimentally testable in the near future.

## 1. Introduction

The current data on exclusive  $b \rightarrow s\mu^+\mu^-$  processes have exhibited several tantalizing deviations from what the standard model (SM) of particle physics predicts [1]. Although their statistical significance is still too low for making a conclusive inference, these anomalous results may be initial revelations about the existence of new physics (NP) in the quark sector. As a matter of fact, model-independent theoretical studies have indicated that NP could explain them [2, 3], which perhaps suggests that these anomalies may be empirically established to have arisen from beyond the SM not too long from now. Therefore, it is an opportune time to consider what if the same NP could importantly impact some other  $b \rightarrow s$  processes.

In what follows, we present the main results of our recent work [4, 5] exploring such a possibility in a scenario where a new, colorless and electrically neutral, spin-one particle, the  $Z'$  boson, is responsible for the anomalies by virtue of its family-nonuniversal and flavor-changing interactions with SM fermions. We examine specifically what this might imply for the nonleptonic two-body modes  $\bar{B}_s \rightarrow (\eta, \eta', \phi)(\pi^0, \rho^0, \omega)$ , the majority of which have not yet been observed [6]. In the SM, the amplitudes for these decays are induced by  $b \rightarrow s$  four-quark operators  $O_{1,2}^u$ ,  $O_{3,4,5,6}$ , and  $O_{7,8,9,10}$  which proceed from charmless tree, QCD-penguin, and electroweak-penguin diagrams, respectively. Since the influence of  $O_{1,2}^u$  on these transitions is suppressed by a factor  $|V_{us}V_{ub}|/|V_{ts}V_{tb}| \sim 0.02$  involving the elements of the Cabibbo-Kobayashi-Maskawa (CKM) matrix, the amplitudes tend to be dominated by the penguin contributions. Accordingly, their rates in the SM are estimated to be comparatively low [7, 8, 9, 10, 11, 12, 13].

This motivated earlier analyses proposing that one or more of these  $\bar{B}_s$  modes could be sensitive to NP signals [14, 15, 16, 17, 18, 19, 20].

## 2. Interactions

In many extensions of the SM, new ingredients may alter the Wilson coefficients  $C_i$  of  $O_i$  and/or bring about extra operators  $\tilde{O}_i$ , which are the chirality-flipped counterparts of  $O_i$ . (The formulas for  $O_{1,2,\dots,10}$  can be found in, *e.g.*, ref. [13].) If a  $Z'$  boson possesses flavor-changing quark couplings, it may contribute at tree level to part or all of the penguin sector, depending on the details of the  $Z'$  properties.

In this study, the relevant interactions of the  $Z'$  with the mass eigenstates of the  $u$ ,  $d$ ,  $s$ , and  $b$  quarks can be expressed as [4]

$$\mathcal{L}_{Z'} \supset -[\bar{s}Z'(\Delta_L^{sb}P_L + \Delta_R^{sb}P_R)b + \text{H.c.}] - \bar{u}Z'(\Delta_L^{uu}P_L + \Delta_R^{uu}P_R)u - \bar{d}Z'(\Delta_L^{dd}P_L + \Delta_R^{dd}P_R)d - \Delta_V^{\mu\mu}\bar{\mu}Z'\mu, \quad (1)$$

where  $\Delta_{L,R}^{sb}$  are generally complex constants, whereas  $\Delta_V^{\mu\mu}$  and  $\Delta_{L,R}^{uu,dd}$  are real parameters because of the Hermiticity of  $\mathcal{L}_{Z'}$ , and  $P_{L,R} = (1 \mp \gamma_5)/2$ . We suppose that any other possible interactions of the  $Z'$  with SM fermions are negligible and that it has no mixing with SM gauge bosons but does not have to be a gauge boson. Furthermore, for the sake of simplicity we concentrate on the case in which the  $Z'$  is heavy and  $\Delta_{L,R}^{sb} = \rho_{L,R}V_{ts}^*V_{tb}$  with real  $\rho_{L,R}$ .

Evidently, the  $Z'$  couplings to  $b\bar{s}$  and  $\mu\bar{\mu}$  in eq. (1) give rise to the diagram depicted in figure 1. In the limit that the  $Z'$  mass,  $m_{Z'}$ , is large, this translates into NP contributions to the effective interactions behind  $b \rightarrow s\mu^+\mu^-$  described by

$$\mathcal{L}_{\text{eff}} \supset \frac{\alpha_e \lambda_t G_F}{\sqrt{2}\pi} (C_{9\mu} \bar{s} \gamma^\kappa P_L b + C_{9'\mu} \bar{s} \gamma^\kappa P_R b) \bar{\mu} \gamma_\kappa \mu + \text{H.c.}, \quad (2)$$

where  $\alpha_e$  and  $G_F$  represent the fine-structure and Fermi constants, respectively,  $\lambda_q = V_{qs}^*V_{qb}$ , and the Wilson coefficients are given by [4]

$$C_{9\mu} = C_{9\ell}^{\text{SM}} + C_{9\mu}^{\text{NP}}, \quad C_{9\mu}^{\text{NP}} = \frac{-\sqrt{2}\pi\rho_L\Delta_V^{\mu\mu}}{\alpha_e G_F m_{Z'}^2}, \quad C_{9'\mu} = C_{9'\mu}^{\text{NP}} = \frac{-\sqrt{2}\pi\rho_R\Delta_V^{\mu\mu}}{\alpha_e G_F m_{Z'}^2}, \quad (3)$$

with  $C_{9\ell}^{\text{SM}}$  being the lepton-flavor-universal SM part. We remark that  $b \rightarrow s\mu^+\mu^-$  operators with chiral structures different from those in eq. (2) could occur in other  $Z'$  scenarios, such as the one in ref. [21].

As mentioned earlier, physics beyond the SM can modify the Wilson coefficients  $C_j$  of the four-quark operators  $O_j$  pertaining to  $\bar{B}_s \rightarrow (\eta, \eta', \phi)(\pi^0, \rho^0, \omega)$  and/or generate new operators  $\tilde{O}_j$  which are the chirality-flipped counterparts of  $O_j$ , have coefficients  $\tilde{C}_j$ , and contribute to these same transitions. In particular,  $\mathcal{L}_{Z'}$  in eq. (1), via the diagram shown in figure 2, impacts

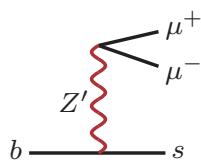


**Figure 1.** The  $Z'$ -mediated diagram contributing to  $b \rightarrow s\mu^+\mu^-$ .

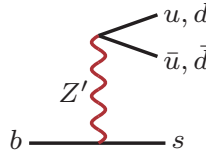


**Figure 2.** The  $Z'$ -mediated diagram contributing to  $b \rightarrow sq\bar{q}$  for  $q = u, d$ .

$C_{3,5,7,9}$  and  $\tilde{C}_{3,5,7,9}$  at the  $W$ -mass scale according to [14, 15, 19]

$$\mathcal{L}_{\text{eff}} \supset \sqrt{8} \lambda_t G_F \sum_{q=u,d} \left\{ \bar{s} \gamma^\kappa P_L b \left[ \left( C_3 + \frac{3}{2} C_9 e_q \right) \bar{q} \gamma_\kappa P_L q + \left( C_5 + \frac{3}{2} C_7 e_q \right) \bar{q} \gamma_\kappa P_R q \right] + \bar{s} \gamma^\kappa P_R b \left[ \left( \tilde{C}_3 + \frac{3}{2} \tilde{C}_9 e_q \right) \bar{q} \gamma_\kappa P_R q + \left( \tilde{C}_5 + \frac{3}{2} \tilde{C}_7 e_q \right) \bar{q} \gamma_\kappa P_L q \right] \right\}, \quad (4)$$

where  $C_i = C_i^{SM} + C_i^{Z'}$  and  $\tilde{C}_i = \tilde{C}_i^{Z'}$  for  $i = 3, 5, 7, 9$  with [4]

$$\begin{aligned} C_{3,5}^{Z'} &= \frac{\rho_L (-\delta_{L,R} - 3\Delta_{L,R}^{dd})}{6\sqrt{2} G_F m_{Z'}^2}, & C_{7,9}^{Z'} &= \frac{-\rho_L \delta_{R,L}}{3\sqrt{2} G_F m_{Z'}^2}, \\ \tilde{C}_{3,5}^{Z'} &= \frac{\rho_R (-\delta_{R,L} - 3\Delta_{R,L}^{dd})}{6\sqrt{2} G_F m_{Z'}^2}, & \tilde{C}_{7,9}^{Z'} &= \frac{-\rho_R \delta_{L,R}}{3\sqrt{2} G_F m_{Z'}^2}, \end{aligned} \quad (5)$$

where  $\delta_{L,R} = \Delta_{L,R}^{uu} - \Delta_{L,R}^{dd}$  and we have assumed that the effects of renormalization group evolution (RGE) between the  $m_{Z'}$  and  $m_W$  scales are negligible. At the  $b$ -quark mass scale, all the penguin coefficients gain  $Z'$  contributions via RGE, which will be taken into account in our numerical analysis.

### 3. Decay amplitudes

To evaluate  $\bar{B}_s \rightarrow M_1 M_2$ , where  $M_1 M_2$  can be pseudoscalars ( $PP'$ ), vectors ( $VV'$ ), or  $PV$ , we adopt the framework of soft-collinear effective theory (SCET) following refs. [11, 12, 13]. In SCET the amplitude for each of these decays at leading order in the strong coupling  $\alpha_s(m_b)$  can be written as [12]

$$\begin{aligned} \mathcal{A}_{\bar{B}_s \rightarrow M_1 M_2} &= \frac{f_{M_1} G_F m_{B_s}^2}{\sqrt{2}} \left[ \int_0^1 d\nu \left( \zeta_J^{BM_2} T_{1J}(\nu) + \zeta_{Jg}^{BM_2} T_{1Jg}(\nu) \right) \phi_{M_1}(\nu) + \zeta^{BM_2} T_1 + \zeta_g^{BM_2} T_{1g} \right] \\ &+ (1 \leftrightarrow 2), \end{aligned} \quad (6)$$

where  $f_M$  stands for the decay constant of meson  $M$ , the  $\zeta$ s represent nonperturbative hadronic parameters which can be experimentally determined, the  $T$ s are hard kernels which depend on the Wilson coefficients  $C_j$  and  $\tilde{C}_j$  at the  $m_b$  scale, and  $\phi_M(\nu)$  is the light-cone distribution amplitude of  $M$  which are normalized as  $\int_0^1 d\nu \phi_M(\nu) = 1$ . Formulas for the  $T$ s are available from refs. [11, 12, 13] and listed in table 1, where the flavor states  $\eta_q \sim (u\bar{u} + d\bar{d})/\sqrt{2}$  and  $\eta_s \sim s\bar{s}$  are connected to the physical mesons  $\eta$  and  $\eta'$  by  $\eta = \eta_q \cos \theta - \eta_s \sin \theta$  and  $\eta' = \eta_q \sin \theta + \eta_s \cos \theta$  with mixing angle  $\theta = 39.3^\circ$  [12, 13, 22, 23]. For  $\bar{B}_s \rightarrow (\eta_q, \eta_s) \pi^0$  and  $\bar{B}_s \rightarrow \phi(\rho^0, \omega)$ , the Wilson coefficients are contained in

$$c_2 = \lambda_u \left( C_2^- + \frac{C_1^-}{N_c} \right) - \frac{3\lambda_t}{2} \left( C_9^- + \frac{C_{10}^-}{N_c} \right), \quad c_3 = -\frac{3\lambda_t}{2} \left( C_7^- + \frac{C_8^-}{N_c} \right),$$

**Table 1.** The hard kernels  $T_{1,2,1g,2g}$  for  $\bar{B}_s \rightarrow (\eta, \eta', \phi)(\pi^0, \rho^0, \omega)$ . The hard kernels  $T_{rJ,rJg}(\nu)$  for  $r = 1, 2$  equal  $T_{r,rg}$ , respectively, but with  $c_k$  replaced by  $b_k$ , where  $b_k$  has dependence on  $\nu$ .

Decay mode	$T_1$	$T_2$	$T_{1g}$	$T_{2g}$
$\bar{B}_s \rightarrow \eta_s \pi^0$	0	$\frac{1}{\sqrt{2}}(c_2 - c_3)$	0	$\frac{1}{\sqrt{2}}(c_2 - c_3)$
$\bar{B}_s \rightarrow \eta_s \rho^0$	0	$\frac{1}{\sqrt{2}}(c_2 + c_3)$	0	$\frac{1}{\sqrt{2}}(c_2 + c_3)$
$\bar{B}_s \rightarrow \eta_q \pi^0$	0	0	0	$c_2 - c_3$
$\bar{B}_s \rightarrow \eta_q \rho^0$	0	0	0	$c_2 + c_3$
$\bar{B}_s \rightarrow \phi \pi^0$	0	$\frac{1}{\sqrt{2}}(c_2 - c_3)$	0	0
$\bar{B}_s \rightarrow \phi \rho^0$	0	$\frac{1}{\sqrt{2}}(c_2 + c_3)$	0	0
$\bar{B}_s \rightarrow \eta_s \omega$	0	$\frac{1}{\sqrt{2}}(c_2 + c_3 + 2c_5 + 2c_6)$	0	$\frac{1}{\sqrt{2}}(c_2 + c_3 + 2c_5 + 2c_6)$
$\bar{B}_s \rightarrow \eta_q \omega$	0	0	0	$c_2 + c_3 + 2c_5 + 2c_6$
$\bar{B}_s \rightarrow \phi \omega$	0	$\frac{1}{\sqrt{2}}(c_2 + c_3 + 2c_5 + 2c_6)$	0	0

$$c_{5,6} = -\lambda_t \left( C_{3,5}^- + \frac{C_{4,6}^-}{N_c} - \frac{C_{9,7}^-}{2} - \frac{C_{10,8}^-}{2N_c} \right), \quad (7)$$

$$b_2 = \lambda_u \left[ C_2^- + \left( 1 - \frac{m_b}{\omega_3} \right) \frac{C_1^-}{N_c} \right] - \frac{3\lambda_t}{2} \left[ C_9^- + \left( 1 - \frac{m_b}{\omega_3} \right) \frac{C_{10}^-}{N_c} \right],$$

$$b_3 = -\frac{3\lambda_t}{2} \left[ C_7^- + \left( 1 - \frac{m_b}{\omega_2} \right) \frac{C_8^-}{N_c} \right],$$

$$b_{5,6} = -\lambda_t \left[ C_{3,5}^- + \left( 1 - \frac{m_b}{\omega_3} \right) \frac{C_{4,6}^-}{N_c} - \frac{C_{9,7}^-}{2} - \left( 1 - \frac{m_b}{\omega_3} \right) \frac{C_{10,8}^-}{2N_c} \right], \quad (8)$$

where  $C_j^- = C_j - \tilde{C}_j$ , the color number  $N_c = 3$ , and  $b_{2,3,5,6}$ , which occur in  $T_{2J,2Jg}(\nu)$ , are also functions of  $\nu$  through  $\omega_2 = \nu m_{B_s}$  and  $\omega_3 = (\nu - 1)m_{B_s}$ . However, for  $\bar{B}_s \rightarrow (\eta_q, \eta_s)(\rho^0, \omega)$  and  $\bar{B}_s \rightarrow \phi \pi^0$ , one needs to apply the sign change  $C_j^- \rightarrow C_j^+ = C_j + \tilde{C}_j$  in  $c_{2,3,5,6}$  and  $b_{2,3,5,6}$ . In  $C_j$  and  $\tilde{C}_j$  we take into account the effects of RGE at leading-logarithm order [24] between the  $m_W$  and  $m_b$  scales, with  $\alpha_e = 1/128$ ,  $\alpha_s(m_Z) = 0.119$ ,  $m_b = 4.8$  GeV, and  $m_t = 174.3$  GeV [13]. The choices for other parameters needed to obtain the following numerical results are detailed further in [5].

#### 4. Numerical analysis

Combining the SM and  $Z'$  portions of the amplitudes for  $\bar{B}_s \rightarrow (\eta, \eta')(\pi^0, \rho^0, \omega)$  in the form

$$\mathcal{A}_{\bar{B}_s \rightarrow M_1 M_2}^{(r)} = \mathcal{A}_{M_1 M_2}^{(r)SM} + \hat{\mathcal{A}}_{M_1 M_2}^{(r)}, \quad r = 1, 2, \quad (9)$$

we find [5], in units of  $10^{-9}$  GeV,

$$\begin{aligned}
 \mathcal{A}_{\eta\pi^0}^{(1)\text{SM}} &= 1.43 + 1.31i, & \mathcal{A}_{\eta\pi^0}^{(2)\text{SM}} &= 1.67 + 0.47i, \\
 \mathcal{A}_{\eta'\pi^0}^{(1)\text{SM}} &= -0.31 - 0.21i, & \mathcal{A}_{\eta'\pi^0}^{(2)\text{SM}} &= 0.48 - 2.48i, \\
 \mathcal{A}_{\phi\pi^0}^{(1)\text{SM}} &= -1.63 - 2.53i, & \mathcal{A}_{\phi\pi^0}^{(2)\text{SM}} &= -2.88 - 1.69i, \\
 \mathcal{A}_{\eta\rho^0}^{(1)\text{SM}} &= 2.18 + 2.17i, & \mathcal{A}_{\eta\rho^0}^{(2)\text{SM}} &= 2.56 + 0.77i, \\
 \mathcal{A}_{\eta'\rho^0}^{(1)\text{SM}} &= -0.47 - 0.34i, & \mathcal{A}_{\eta'\rho^0}^{(2)\text{SM}} &= 0.78 - 4.12i, \\
 \mathcal{A}_{\eta\omega}^{(1)\text{SM}} &= -0.63 + 2.05i, & \mathcal{A}_{\eta\omega}^{(2)\text{SM}} &= 0.52 + 0.74i, \\
 \mathcal{A}_{\eta'\omega}^{(1)\text{SM}} &= 0.05 - 0.33i, & \mathcal{A}_{\eta'\omega}^{(2)\text{SM}} &= 3.23 - 3.83i
 \end{aligned} \tag{10}$$

and the  $Z'$  contributions

$$\begin{aligned}
 \hat{\mathcal{A}}_{\eta\pi^0}^{(1)} &= 0.03 \delta_+ \rho_- + (4.15 - 0.08i) \delta_- \rho_+, & \hat{\mathcal{A}}_{\eta\pi^0}^{(2)} &= (3.98 - 0.08i) \delta_- \rho_+, \\
 \hat{\mathcal{A}}_{\eta'\pi^0}^{(1)} &= -(0.84 - 0.02i) \delta_- \rho_+, & \hat{\mathcal{A}}_{\eta'\pi^0}^{(2)} &= -0.09 \delta_+ \rho_- - (1.0 - 0.02i) \delta_- \rho_+, \\
 \hat{\mathcal{A}}_{\phi\pi^0}^{(1)} &= -(5.57 - 0.11i) \delta_- \rho_- - 0.08 \delta_+ \rho_+, & \hat{\mathcal{A}}_{\phi\pi^0}^{(2)} &= -(7.58 - 0.15i) \delta_- \rho_- - 0.03 \delta_+ \rho_+, \\
 \hat{\mathcal{A}}_{\eta\rho^0}^{(1)} &= 0.06 \delta_- \rho_- + (6.6 - 0.13i) \delta_+ \rho_+, & \hat{\mathcal{A}}_{\eta\rho^0}^{(2)} &= (6.35 - 0.12i) \delta_+ \rho_+, \\
 \hat{\mathcal{A}}_{\eta'\rho^0}^{(1)} &= -0.01 \delta_- \rho_- - (1.33 - 0.03i) \delta_+ \rho_+, & \hat{\mathcal{A}}_{\eta'\rho^0}^{(2)} &= -0.16 \delta_- \rho_- - (1.52 - 0.03i) \delta_+ \rho_+, \\
 \hat{\mathcal{A}}_{\eta\omega}^{(1)} &= [(6.06 - 0.12i) \delta_+ + (12.1 - 0.23i) \Delta_+] \rho_+ + (0.02 \delta_- + 0.01 \Delta_-) \rho_-, & \\
 \hat{\mathcal{A}}_{\eta\omega}^{(2)} &= [(5.83 - 0.11i) \delta_+ + (11.7 - 0.22i) \Delta_+] \rho_+ + 0.01 \Delta_- \rho_-, & \\
 \hat{\mathcal{A}}_{\eta'\omega}^{(1)} &= -[(1.22 - 0.02i) \delta_+ + (2.44 - 0.05i) \Delta_+] \rho_+, & \\
 \hat{\mathcal{A}}_{\eta'\omega}^{(2)} &= -[(1.37 - 0.03i) \delta_+ + (2.72 - 0.05i) \Delta_+] \rho_+ - (0.05 \delta_- + 0.01 \Delta_-) \rho_-
 \end{aligned} \tag{11}$$

where the superscripts (1) and (2) refer, respectively, to the two sets (hereafter designated Solution 1 and Solution 2) of SCET parameters which we have employed and which were determined in [12] from fitting to  $b$ -meson data,  $\delta_{\pm} = \delta_L \pm \delta_R$ , and  $\rho_{\pm} = \rho_L \pm \rho_R$ . For  $\bar{B}_s \rightarrow \phi \rho^0, \phi \omega$  the amplitudes are [5]

$$\mathcal{A}_{\bar{B}_s \rightarrow \phi \rho^0} \simeq -6.53 - 1.47i + 0.01 \delta_- \rho_+ - (15.5 - 0.29i) \delta_+ \rho_-, \tag{12}$$

$$\mathcal{A}_{\bar{B}_s \rightarrow \phi \omega} \simeq -1.69 - 1.41i - (0.01 \delta_- + 0.03 \Delta_-) \rho_+ - [(14 - 0.26i) \delta_+ + (28.1 - 0.53i) \Delta_+] \rho_- \tag{13}$$

in units of  $10^{-9}$  GeV.

In the absence of the  $Z'$  parts, the above amplitudes lead to the predictions for the branching fractions within the SM. In tables 2 and 3, under the ‘SCET’ headings, we put together the results we reported in refs. [4, 5], which also provide explanations for the theoretical uncertainties. For comparison, in the tables we include the corresponding values obtained with the QCD factorization (QCDF) and perturbative QCD (PQCD) approaches in the literature [9, 10, 25, 26]. The displayed SCET numbers turn out to be roughly similar to their QCDF and PQCD counterparts within sizable errors. The important implication is that for NP influence to be unambiguously detectable in the rates it would have to magnify them with respect to their SM ranges by much more than factors of two.

**Table 2.** The SM predictions for the branching fractions of  $\bar{B}_s \rightarrow (\eta, \eta')(\pi^0, \rho^0, \omega)$  and  $\bar{B}_s \rightarrow \phi\pi^0$  in units of  $10^{-6}$ . The second and third columns exhibit the numbers evaluated in refs. [4, 5] under the SCET framework, and the ones in the last two columns were computed with QCDF [9] and PQCD [10, 25].

Decay mode	SCET Solution 1	SCET Solution 2	QCDF	PQCD
$\bar{B}_s \rightarrow \eta\pi^0$	$0.032 \pm 0.015$	$0.025 \pm 0.010$	$0.05^{+0.03+0.02}_{-0.01-0.01}$	$0.05^{+0.02+0.01+0.00}_{-0.02-0.01-0.00}$
$\bar{B}_s \rightarrow \eta'\pi^0$	$0.001 \pm 0.005$	$0.052 \pm 0.026$	$0.04^{+0.01+0.01}_{-0.00-0.00}$	$0.11^{+0.05+0.02+0.00}_{-0.03-0.01-0.00}$
$\bar{B}_s \rightarrow \phi\pi^0$	$0.074 \pm 0.031$	$0.091 \pm 0.040$	$0.12^{+0.02+0.04}_{-0.01-0.02}$	$0.16^{+0.06+0.02+0}_{-0.05-0.02-0}$
$\bar{B}_s \rightarrow \eta\rho^0$	$0.078 \pm 0.038$	$0.059 \pm 0.024$	$0.10^{+0.02+0.02}_{-0.01-0.01}$	$0.06^{+0.03+0.01+0.00}_{-0.02-0.01-0.00}$
$\bar{B}_s \rightarrow \eta'\rho^0$	$0.003 \pm 0.013$	$0.141 \pm 0.070$	$0.16^{+0.06+0.03}_{-0.02-0.03}$	$0.13^{+0.06+0.02+0.00}_{-0.04-0.02-0.01}$
$\bar{B}_s \rightarrow \eta\omega$	$0.04^{+0.04}_{-0.02}$	$0.007^{+0.011}_{-0.002}$	$0.03^{+0.12+0.06}_{-0.02-0.01}$	$0.11^{+0.04}_{-0.03}$
$\bar{B}_s \rightarrow \eta'\omega$	$0.001^{+0.095}_{-0.000}$	$0.20^{+0.34}_{-0.17}$	$0.15^{+0.27+0.15}_{-0.08-0.06}$	$0.35^{+0.06}_{-0.04}$

**Table 3.** The SM predictions for the branching fractions of  $\bar{B}_s \rightarrow \phi(\rho^0, \omega)$  in units of  $10^{-6}$ . The second column contains the numbers calculated in refs. [4, 5] under the SCET framework, and those in the last two columns were computed with QCDF [9] and PQCD [26].

Decay mode	SCET	QCDF	PQCD
$\bar{B}_s \rightarrow \phi\rho^0$	$0.36 \pm 0.15$	$0.18^{+0.01+0.09}_{-0.01-0.04}$	$0.25^{+0.18}_{-0.11}$
$\bar{B}_s \rightarrow \phi\omega$	$0.04 \pm 0.01$	$0.18^{+0.44+0.47}_{-0.12-0.04}$	$0.22^{+0.15}_{-0.10}$

Keeping the non-SM terms in the amplitudes, as discussed in refs. [4, 5], we need to ensure that the  $Z'$  couplings comply with the various pertinent constraints, which we list here. Firstly, the products  $\rho_{L,R} \Delta_V^{\mu\mu}$  must be compatible with the detected  $b \rightarrow s\mu^+\mu^-$  anomalies, which prefer NP manifestations in the muonic coefficients,  $C_{9\mu}^{\text{NP}} \sim -1.1$  and  $C_{9'\mu}^{\text{NP}} \sim 0.4$  in eq. (3), with no NP in  $b \rightarrow se^+e^-$ , according to the model-independent analyses done in refs. [2, 3]. Secondly,  $\Delta_{L,R}^{sb} = \rho_{L,R} V_{ts}^* V_{tb}$  affect  $B_s$ - $\bar{B}_s$  mixing at tree level, through the diagrams depicted in figure 3, and hence have to be consistent with its data as well. These two requisites together entail the

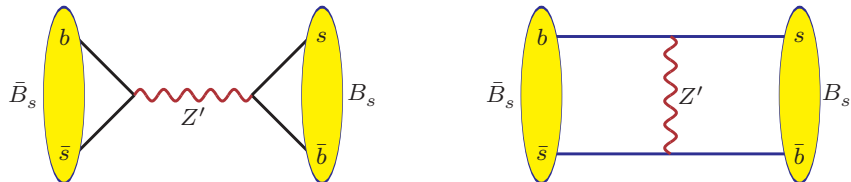


**Figure 3.** The  $Z'$ -mediated diagrams contributing to  $B_s$ - $\bar{B}_s$  mixing.

condition  $\Delta_L^{sb} \sim 10\Delta_R^{sb}$ , which translates into  $\rho_L \sim 10\rho_R$ . For definiteness we pick  $\rho_R = 0.1\rho_L$  and the  $Z'$  mass  $m_{Z'} = 1$  TeV in the following. Thirdly, additional restraints are supplied by the experimental evidence for  $\bar{B}_s \rightarrow \phi\rho^0$ , which has a branching fraction [6] in agreement with its SM estimates [9, 10, 11], and by the data on other nonleptonic  $b \rightarrow s$  processes which have been observed. Concerning the latter, we focus on the well-measured decays  $B^- \rightarrow \pi^0 K^-, \pi^- \bar{K}^0$  and  $\bar{B}^0 \rightarrow \pi^0 \bar{K}^0, \pi^+ K^-$  plus their antiparticle counterparts. Lastly, we also take into account restrictions inferred from collider measurements.

To illustrate how the  $Z'$  interactions contribute to the decays of interest, we collect 5,000 randomly generated benchmarks fulfilling the aforementioned requirements, with more details given in ref. [5]. We exhibit the main results in the remaining figures, which show two-dimensional projections of the benchmarks for several quantities.

In figure 4 we graph the distributions of the enhancement factor

$$\mathcal{R}(M_1 M_2) = \frac{\Gamma_{\bar{B}_s \rightarrow M_1 M_2}}{\Gamma_{\bar{B}_s \rightarrow M_1 M_2}^{\text{SM}}} \quad (14)$$

of the  $\bar{B}_s \rightarrow M_1 M_2$  rate with respect to its SM prediction, for a few pairs of final states  $M_1 M_2$ . As the top-left plot indicates,  $\mathcal{R}(\eta\omega)$  and  $\mathcal{R}(\phi\omega)$  rise and fall at the same time and can grow up to roughly 50 and 150 (270 and 170), respectively, if the Solution 1 (2) SCET parameters are used. In other words, the  $Z'$  impact can amplify the rates of  $\bar{B}_s \rightarrow \eta\omega, \phi\omega$  by up to two orders of magnitude above their SM expectations. Accordingly, these decay channels can be valuable probes for this kind of  $Z'$ , and moreover the correlation between  $\mathcal{R}(\eta\omega)$  and  $\mathcal{R}(\phi\omega)$  may be experimentally checked.

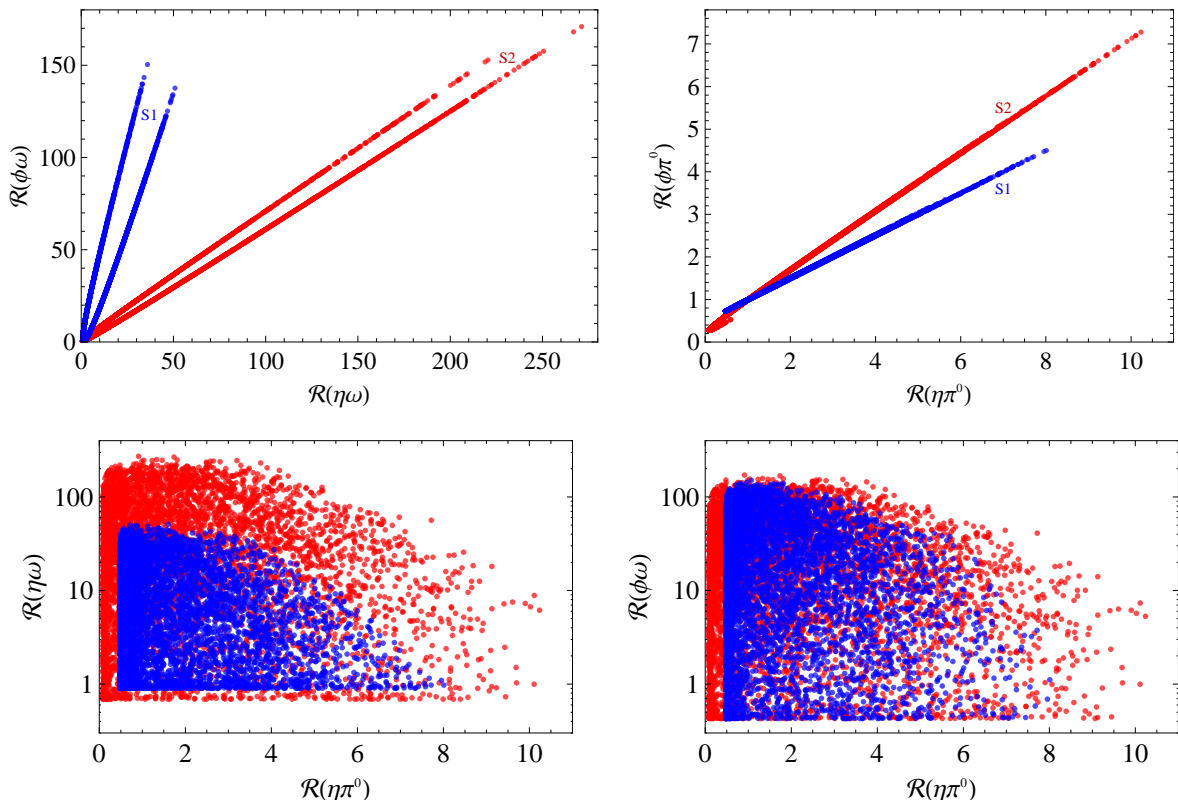


**Figure 4.** The distributions of  $\mathcal{R}(M_1 M_2) = \Gamma_{\bar{B}_s \rightarrow M_1 M_2} / \Gamma_{\bar{B}_s \rightarrow M_1 M_2}^{\text{SM}}$  among different pairs of final states  $M_1 M_2$  for the benchmarks corresponding to Solutions 1 (blue, S1) and 2 (red, S2).

From the top-right plot in figure 4, we learn that  $\mathcal{R}(\eta\pi^0)$  and  $\mathcal{R}(\phi\pi^0)$ , like  $\mathcal{R}(\eta\omega)$  and  $\mathcal{R}(\phi\omega)$ , go up and down simultaneously, but the former two cannot exceed about 8.0 and 4.5 (10 and 7.3), respectively, for Solution 1 (2). Nevertheless, as elaborated in ref. [4], such enhancement factors are big enough to make  $\bar{B}_s \rightarrow \eta\pi^0, \phi\pi^0$  promising as extra tools in the search for the potential NP behind the  $b \rightarrow s\mu^+\mu^-$  anomalies. Evidently, the correlation between  $\mathcal{R}(\eta\pi^0)$  and  $\mathcal{R}(\phi\pi^0)$  is a prediction which can be empirically tested as well.

Information regarding relationships between  $\mathcal{R}(M_1 M_2)$  and the  $Z'$  couplings is greatly valuable for examining the latter if one or more of these decays are discovered. For our modes of highest interest, it turns out that there are a few relationships that are more or less simple to see, which we display in figure 5.

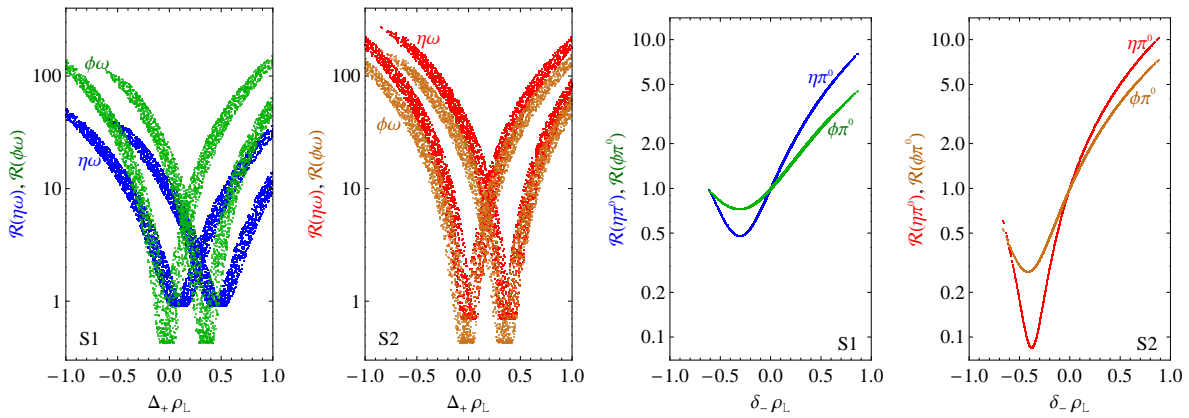


**Figure 5.** The distributions of  $\mathcal{R}(\eta\omega)$  and  $\mathcal{R}(\phi\omega)$  versus  $\Delta_+\rho_L$  and of  $\mathcal{R}(\eta\pi^0)$  and  $\mathcal{R}(\phi\pi^0)$  versus  $\delta_-\rho_L$  for Solutions 1 (S1) and 2 (S2).

## 5. Conclusions

We have entertained the possibility that the anomalous features uncovered in the data from the latest  $b \rightarrow s\mu^+\mu^-$  measurements are caused by physics beyond the SM and that the same underlying NP influences the rare nonleptonic decays of the  $\bar{B}_s$  meson which tend to be dominated by penguin contributions. Specifically, we consider a scenario in which the anomalies arise from the presence of a heavy  $Z'$  boson with family-nonuniversal and flavor-violating quark interactions and investigate the implications for  $\bar{B}_s \rightarrow (\eta, \eta', \phi)(\pi^0, \rho^0, \omega)$ . The majority of these modes are still unobserved and in the SM their rates are relatively low, which makes them potentially good places to look for manifestations of NP. Taking into account the relevant constraints, we demonstrate that the  $Z'$  effects could boost the rates of four of these channels tremendously with respect to their SM predictions, particularly  $\bar{B}_s \rightarrow (\eta, \phi)\pi^0$  and  $\bar{B}_s \rightarrow (\eta, \phi)\omega$  by factors of order 10 and 100, respectively. Thus, these decays could be consequential should future experimental efforts establish that the current  $b \rightarrow s\mu^+\mu^-$  anomalies are really NP signals. Quests for  $\bar{B}_s \rightarrow (\eta, \phi)(\pi^0, \omega)$  would therefore be highly desirable, which may be conducted in the LHCb and perhaps also Belle II experiments.

## Acknowledgments

This research was supported in part by the Taiwan Ministry of Science and Technology (Grant No. MOST 106-2112-M-002-003-MY3).

## References

[1] Aaij R *et al.* *Preprint* arXiv:1808.08865

- [2] Capdevila B *et al.* 2018 *J. High Energy Phys.* JHEP01(2018)093
- [3] Altmannshofer W, Stangl P and Straub D M 2017 *Phys. Rev. D* **96** 055008
- [4] Faisel G and Tandean J 2018 *J. High Energy Phys.* JHEP02(2018)074 (*Preprint* arXiv:1710.11102)
- [5] Faisel G and Tandean J 2019 *Phys. Rev. D* **99** 075007 (*Preprint* arXiv:1810.11437)
- [6] Tanabashi M *et al.* 2018 *Phys. Rev. D* **98** 030001
- [7] Fleischer R 1994 *Phys. Lett. B* **332** 419
- [8] Deshpande N G, He X G and Trampetic J 1995 *Phys. Lett. B* **345** 547
- [9] Cheng H Y and Chua C K 2009 *Phys. Rev. D* **80** 114026
- [10] Ali A *et al.* 2007 *Phys. Rev. D* **76** 074018
- [11] Wang C *et al.* 2017 *Phys. Rev. D* **96** 073004
- [12] Wang W *et al.* 2008 *Phys. Rev. D* **78** 034011
- [13] Williamson A R and Zupan J 2006 *Phys. Rev. D* **74** 014003; (*Erratum*) 03901
- [14] Hua J, Kim C S and Li Y 2010 *Phys. Lett. B* **690** 508
- [15] Hofer L, Scherer D and Vernazza L 2011 *J. High Energy Phys.* JHEP02(2011)080
- [16] Faisel G 2012 *J. High Energy Phys.* JHEP08(2012)031
- [17] Faisel G 2014 *Phys. Lett. B* 279
- [18] Faisel G 2017 *Eur. Phys. J. C* **77** 380
- [19] Chang Q, Li X Q and Yang Y D 2014 *J. Phys. G* **41** 105002
- [20] Bobeth C, Gorbahn M and Vickers S 2015 *Eur. Phys. J. C* **75** 340
- [21] Chiang C W, He X G, Tandean J and Yuan X B 2017 *Phys. Rev.* **96** 115022
- [22] Feldmann T, Kroll P and Stech B 1998 *Phys. Rev. D* **58** 114006
- [23] Feldmann T, Kroll P and Stech B 1999 *Phys. Lett. B* **449** 339
- [24] Buchalla G, Buras A J and Lautenbacher M E 1996 *Rev. Mod. Phys.* **68** 1125
- [25] Yan D C *et al.* 2018 *Nucl. Phys. B* **931** 79
- [26] Yan D C *et al.* 2018 *Nucl. Phys. B* **935** 17